Chapter 4
Oligomeric and Polymeric Ionic Liquids: Engineering Architecture and Morphology

Alexandr V. Stryutsky, Volodymyr F. Korolovych, Hansol Lee, Emily Mikan, Andrew Erwin, Oleh O. Sobko, Maryana A. Gumenna, Nina S. Klimenko, Valery V. Shevchenko, Leonid A. Bulavin and Vladimir V. Tsukruk

Abstract The series of amphiphilic anionic protic hyperbranched oligomeric and polymeric ionic liquids (HBP-OILs) with different terminal groups and an adjustable hydrophilic-hydrophobic balance which are sensitive to pH and ionic strength changes was obtained by neutralizing the carboxylic and sulfonic terminal acid groups of aliphatic hyperbranched core with N-methylimidazole (Im) and 1,2,4-1H-triazole (Tr). The introduction of long hydrophobic aliphatic tails to starting hydrophobic hyperbranched core influences more significantly on the size of micellar assemblies than the introduction of ionic groups does. The assembly of these compounds into core-corona micelles in aqueous media in a wide range of pH and ionic conditions was established. Regulation of HBP-OILs amphiphilicity can be realized by varying the extent of ionization of terminal groups by changing pH or ionic strength. The synthesis of the thermally responsive protic anionic hyperbranched poly(ionic liquid)s (HBP-PILs) was based on partial (50%) and full neutralization of carboxyl groups of aliphatic polyester core by monoamine-terminated poly(N-isopropylacrylamide)s (PNIPAM). Its linear oligoester analog was synthesized in a similar way. These compounds possess low critical solution temperature (LCST) behavior with a narrow LCST window and amorphous state in condensed matter. We found that HBP-PILs form smaller in comparison with linear analogues spherical

A. V. Stryutsky (✉) · O. O. Sobko · M. A. Gumenna · N. S. Klimenko · V. V. Shevchenko
Institute of Macromolecular Chemistry of the National Academy of Sciences of Ukraine, Kharkivske Shosse 48, Kyiv 02160, Ukraine
e-mail: striutskyi@gmail.com

V. V. Shevchenko
e-mail: valpshevchenko@gmail.com

V. F. Korolovych · H. Lee · E. Mikan · A. Erwin · V. V. Tsukruk
School of Materials Science and Engineering, Georgia Institute of Technology, Atlanta, GA 30332, USA
e-mail: vladimir@mse.gatech.edu

L. A. Bulavin
Taras Shevchenko National University of Kyiv, Volodymyrska Str. 64, Kyiv 01601, Ukraine
e-mail: bulavin221@gmail.com

L. A. Bulavin and L. Xu (eds.), *Modern Problems of the Physics of Liquid Systems*, Springer Proceedings in Physics 223,
https://doi.org/10.1007/978-3-030-21755-6_4

micelles and their aggregates of different morphologies depending on the content of PNIPAM. When temperature is higher than LCST the formation of spherical micelles, network-like aggregates and large vesicles is observed. In opposite to initial cores prone to form spherical domains the thermally responsive compounds are able to self-assemble into elongated unimolecular nanodomain. The complex self-assembling behavior and diverse morphology of resultant supramolecular assamblies of HBP-OILs and HBP-PILs might lead to unique ionic transport properties as a key point for creation of nanomaterials with tunable ion transport characteristics.

4.1 Introduction

Polymeric analogues of ionic liquids (PILs), obtained on the basis of reactive ionic liquids (ILs), are a new type of polyelectrolytes [1–7]. They combine the unique properties of classical ILs with the possibilities of varying the chemical structure and molecular architecture of polymers. However, these compounds are generally solids below 100 °C with rare exceptions [3–7]. Oligomeric ionic liquids (OILs), which occupy an intermediate state between ILs and PILs by molecular weight, retain the ability to exist in a liquid state at temperatures below 100 °C and combine the advantages of ILs with the peculiarities of the oligomeric state of a mater; in particular, a significant effect of end groups on their properties [3–7]. OILs as a separate class of polymer electrolytes were discussed by our recent study [6].

OILs in analogy with ILs are classified into protic and aprotic, and like PILs, they are also classified into cationic and anionic [2, 8]. In the case of PILs, regardless of the state of aggregation, the distinguishing feature is the presence of so-called ionic-liquid groups (functionalities) in their composition [2, 8, 9]. In terms of molecular architecture, currently existing OILs can be classified into linear, hyperbranched, and star-shaped (as a rule, silsesquioxane) [2, 8]. OILs with various molecular architectures also attract attention as anhydrous ion-conducting media for various electrochemical devices, nanoreactors, complexing agents, bioactive materials and components of optoelectronic devices [2, 8].

Among well-known OILs and PILs, hyperbranched compounds attract considerable attention [4–7]. Hyperbranched compounds are characterized by a globular core-shell structure and a high density of functional end groups on the shell, which opens up broad possibilities for a targeted change in their composition, structure and properties by changing the chemical nature of these groups. The globular structure of macromolecules gives the ability to form guest-host type complexes, provides low viscosity of melts and solutions, greater thermal stability and better solubility in comparison with linear analogues [4–7]. It should be emphasized that the hyperbranched compounds under consideration, as a rule, are oligomers in their nature and characteristics, however, they are known as “hyperbranched polymers” [10].

Introduction of ionic-liquid groups and fragments to the composition of hyperbranched compounds opens up significant opportunities for directional changes in their structure and properties [3]. The cationic protic and aprotic hyperbranched

OILs and PILs are discussed in the literature, while there is only a fragmentary information concerning the anionic representatives [3–7]. Hyperbranched OILs and PILs are capable of self-assembling and forming various hierarchical structures with unique morphology, which are inaccessible to classical ILs. One of the examples of these compounds is amphiphilic cationic hyperbranched OILs and PILs [3, 11]. This assembly behavior makes these compounds promising for the creation of supramolecular functional materials for various purposes [3, 12–14], in particular, membrane structures and liquid crystals [3–7]. Information on the use of these compounds in obtaining self-associated ultrathin films is fragmentary, and the use of the Langmuir-Blodgett (LB) method in obtaining such materials has not been described practically. At the same time, it is known, that such systems are promising in microelectronics, optics, sensor systems, various functionalized surfaces etc. [15, 16]. It should be noted that the LB method is a high-tech method for producing ultrathin films with unique characteristics and precisely adjustable thickness and structure, which opens up broad possibilities in the design of new functional nanomaterials [17–20]. Only a few works have been reported on obtaining the LB films based on linear [21–25] and star-like [25, 26] OILs and PILs. There is no information about LB films based on the OILs and PILs with dendrimeric and hyperbranched structures.

This chapter considers the works of the authors on the synthesis of amphiphilic protic OILs and PILs, the study of the features of formation of supramolecular structures in solution, at interphase boundary and in the condensed state, in particular ultrathin LB films, with response to pH and ionic strength of the environment, as well as temperature.

4.2 Assembly of Amphiphilic Hyperbranched Oligomeric Ionic Liquids in Aqueous Media at Different PH and Ionic Strength, at the Water/Air Interface

This section describes the synthesis of amphiphilic hyperbranched anionic OILs and PILs capable of self-assembling with the formation of various hierarchical structures with response to pH and ionic strength, which makes them promising for use in creating functional materials [3, 12–14]. It should be mentioned that such stimuli-responsive hierarchical structures are known in the absolute majority for non-ionic hyperbranched compounds [11]. However, the information on the application of this approach to hyperbranched OILs and PILs is missing in the literature.

4.2.1 *Synthesis of Amphiphilic Hyperbranched Olymeric Ionic Liquids*

The obtaining the anionic protic hyperbranched oligomeric ionic liquids (HBP-OILs) of amphiphilic type was realized through acylation of a commercially available polyesterpolyol Boltorn®H30 (HBP-OH) by the anhydrides of phthalic or 2-sulfobenzoic acids followed by neutralization of the resultant acidic oligomers with N-methylimidazole (Fig. 4.1) [6].

The hydrophobicity of the compounds was ensured by core type and the hydrophilicity was regulated using different ionic groups. We suggested a way of varying amphiphilicity of these compounds which is to introduce different amount of hydrophobic *n*-octadecylurethane tales to hyperbranched core [4, 5, 7] (Fig. 4.1).

The hydrophilic properties of HBP-OILs was varied by changing ionicity of ionic groups which is dependent on difference in pK_a values of an acid and base used; the ionicity degree increases as the pK_a difference gets larger [4–7]. In our study sulfonate and imidazolium ionic groups exhibited the highest ionicity. The amphiphilicity was controlled by the ratio of the components. Purification of the synthesized HBP-OILs was carried out by precipitation from alcohol into diethyl ether or acetonitrile (the heterocycles used are soluble in these solvents), followed by washing these compounds with the solvents mentioned.

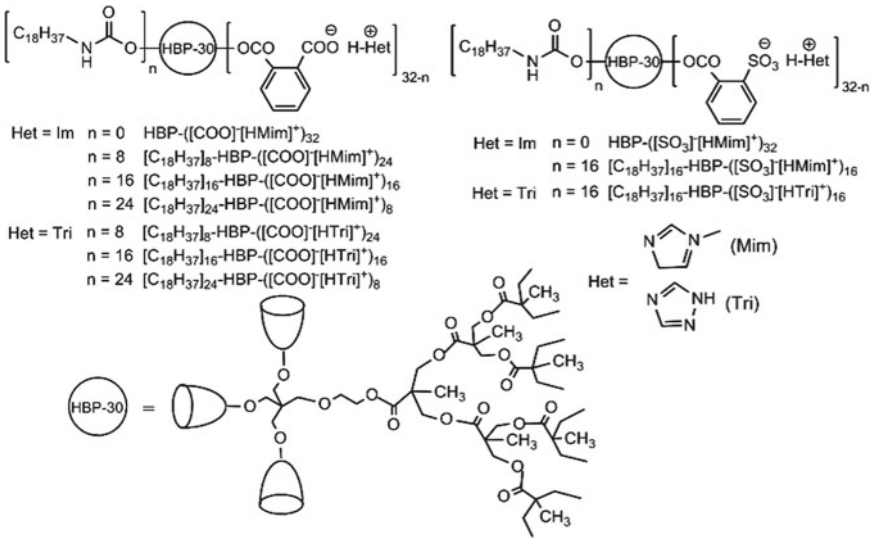

Fig. 4.1 The amphiphilic protic anionic HBP-OILs with adjustable content of different ionic groups and *n*-octadecyl tails. Adapted with permission from [4], copyright (2017) Chemical Society of Japan, [5], copyright (2016) American Chemical Society, and [7, 27], copyright (2017, 2018) Springer Nature

The chemical compositions of the synthesized HBP-OILs are represented in the Fig. 4.1. It should be mentioned that the incorporated alkylurethane substituents can be self-associated by means of Van der Waals interactions and hydrogen bonds. The obtained compounds are viscous liquids at room temperature except HBP-OILs enreached with alkylurethane substituents which are solid below 50–65 °C. The compounds are soluble in polar and insoluble in nonpolar organic solvents.

The experimentally found and calculated values of molecular weight (MW) for the synthesized compounds are in a good agreement (Table 4.1). M_w values obtained from GPC for the compounds $[C_{18}H_{37}]_{24}$-HBP-([COO]_[HMim]$^+$)$_8$ and $[C_{18}H_{37}]_{24}$-HBP-([COO]$^-$[HTri]$^+$)$_8$ are 12,033 g/mol (M_w/M_n = 1.62) and 12,318 g/mol (M_w/M_n = 1.59), respectively. Thermal stability of the synthesized compounds according to TGA data decreases with increase in the content of carboxylate IL groups (Table 4.1). This is due to the low thermal stability of carboxylate IL groups as evidenced by the significantly lower T_d (temperature of onset of thermal-oxidative destruction) value for the compound HBP-([COO]$^-$[HMim]$^+$)$_{32}$ containing only carboxylate imidazolium ionic groups, compared to that of its sulfonate analogue (HBP-([SO$_3$]$^-$[HMim]$^+$)$_{32}$). In accordance with [28], the lower thermal stability of carboxylate IL groups is due to their lower ionicity compared to sulfonate analogues.

As evidenced by DSC method the structure of the obtained compounds depends on the content of ionic groups and alkylurethane substituents (Table 4.1). The compounds with maxima content of ionic groups are amorphous and characterized by the lowest glass-transition temperature (T_g). The T_g value of the HBP-OILs decreases as the ionicity of the ionic groups gets lower (carboxylate-imidazolium HBP-OILs has a lowest T_g). The increase in the content of the aliphatic tales as well as ionicity of the ionic groups is accompanied by the rise in T_g values.

The exceeding of the alkylurethane fragments content above 8 leads to formation of crystalline phase due to the propensity of them to crystalize [7]. The melting point (T_m) of the crystalline phase is a little affected by changing the content of aliphatic tales and composition of ionic groups.

The proton conductivity of the obtained HBP-OILs was established by dielectric relaxation spectroscopy under unhydrous conditions and the highest values was $4.04 \cdot 10^{-4}$ S/cm at 40 °C and $3.22 \cdot 10^{-3}$ S/cm at 120 °C under anhydrous conditions for the compound HBP-([SO$_3$]$^-$[HMim]$^+$)$_{32}$ (Table 4.1) [6]. This is due to the highest content of ionic groups and their iconicity for that compound.

4.2.2 Colloid-Chemical Characteristics and Self-Assembling Peculiarities of Hyperbranched Oligomeric Ionic Liquids in Aqueous Media

Dynamic light scattering (DLS) and AFM data evidence that the obtained HBP-OILs are surfactants able to form micelles and characterized by CMC in the range of 2.4–5.5 mg/mL (Table 4.2). The CMC values of the sulfonate HBP-OILs are

Table 4.1 Characteristics of the synthesized HBP-OILs

Sample	MW		T_d (°C)	T_g (°C)	T_m (°C)	σ_{dc} (S/cm)	
	Found	Calculated				At 40 °C	At 120 °C
HBP-$([COO]^-[HMim]^+)_{32}$	10,112	10,932	145	−16.2	–	$5.60 \cdot 10^{-6}$	$6.95 \cdot 10^{-4}$
$[C_{18}H_{37}]_8$-HBP-$([COO]^-[HMim]^+)_{24}$	12,554	11,626	173	8.9	–	$5.90 \cdot 10^{-8}$	$1.90 \cdot 10^{-4}$
$[C_{18}H_{37}]_8$-HBP-$([COO]^-[HTri]^+)_{24}$	12,241	11,313	192	5.4	–	$7.59 \cdot 10^{-9}$	$5.17 \cdot 10^{-5}$
$[C_{18}H_{37}]_{16}$-HBP-$([COO]^-[HMim]^+)_{16}$	12,386	12,146	198	–	51.2	$4.10 \cdot 10^{-9}$	$1.73 \cdot 10^{-5}$
$[C_{18}H_{37}]_{16}$-HBP-$([COO]^-[HTri]^+)_{16}$	12,177	11,937	228	–	47.3	$1.90 \cdot 10^{-8}$	$3.40 \cdot 10^{-5}$
$[C_{18}H_{37}]_{24}$-HBP-$([COO]^-[HMim]^+)_8$	13,513	12,665	263	–	53.0	$1.30 \cdot 10^{-9}$	$3.70 \cdot 10^{-6}$
$[C_{18}H_{37}]_{24}$-HBP-$([COO]^-[HTri]^+)_8$	13,408	12,560	271	–	52.3	$1.20 \cdot 10^{-10}$	$1.90 \cdot 10^{-7}$
HBP-$([SO_3]^-[HMim]^+)_{32}$	12,951	12,296	270	−9.2	–	$4.04 \cdot 10^{-4}$	$3.22 \cdot 10^{-3}$
$[C_{18}H_{37}]_{16}$-HBP-$([SO_3]^-[HMim]^+)_{16}$	13,314	12,682	294	–	47.0	$1.40 \cdot 10^{-11}$	$1.62 \cdot 10^{-5}$
$[C_{18}H_{37}]_{16}$-HBP-$([SO_3]^-[HTri]^+)_{16}$	13,105	12,473	296	–	51.0	$1.20 \cdot 10^{-11}$	$5.40 \cdot 10^{-6}$

Adapted with permission from [4], copyright (2017) Chemical Society of Japan, [5], copyright (2016) American Chemical Society, and [7, 27], copyright (2017, 2018) Springer Nature

Table 4.2 Colloid-chemical properties of HBP-OILs

Compound	MMA* (nm^2/molecule)	CMC (mg/mL)	Sizes of micelles and their nanoassemblies (nm)				ξ-potential (mV)	
			pH 11.6		pH 5.2		pH 11.6	pH 5.2
			DLS	AFM	DLS	AFM		
$[C_{18}H_{37}]_{16}$-HBP-$([COO]^-[HMim]^+)_{16}$	13.8	$2.4 \cdot 10^{-4}$	12.8 ± 4	15 ± 6	160 ± 50	177 ± 30	−64 ± 7	−56 ± 4
$[C_{18}H_{37}]_{16}$-HBP-$([COO]^-[HTri]^+)_{16}$	14.5	$5.5 \cdot 10^{-4}$	13.7 ± 5	19 ± 8	197 ± 60	207 ± 40	−66 ± 8	−55 ± 4
$[C_{18}H_{37}]_{16}$-HBP-$([SO_3]^-[HMim]^+)_{16}$	16.8	$1.3 \cdot 10^{-4}$	14.0 ± 5	21 ± 10	27 ± 10	30 ± 12	−65 ± 7	−57 ± 4
$[C_{18}H_{37}]_{16}$-HBP-$([SO_3]^-[HTri]^+)_{16}$	18.6	$3.3 \cdot 10^{-4}$	16.4 ± 6	24 ± 12	33 ± 10	37 ± 14	−67 ± 7	−58 ± 4

*MMA is the limiting mean molecular area at water/air interface

Adapted with permission from [4], copyright (2017) Chemical Society of Japan, [5], copyright (2016) American Chemical Society, and [7, 27], copyright (2017, 2018) Springer Nature

40–50% lower compared to that of carboxylate analogs because of less folded state of macromolecules that facilitates hydrogen bonding between urethane groups and therefore stabilization of micelles [5].

It follows from DLS and AFM data that the HBP-OILs form micelles in neutral aqueous solutions two times larger compared to that of starting acid oligomers (12–16 nm vs. 5–7 nm correspondingly) [5]. An increase in pH of aqueous medium has almost no influence on size of micelles because acid groups are in ionized state under these conditions (Figs. 4.2e–h and 4.3, Table 4.2).

A decrease in pH causes micelles aggregation for carboxylate HBP-OILs resulting in formation of 100–250 nm assemblies (Figs. 4.2a, b and 4.3 a, b, Table 4.2).

It should be mentioned that imidazolium compounds form smaller micelles and micelle aggregates in comparison with triazolium analogs because of different ionicity and thus conformations of macromolecules.

The size distribution of the HBP-OILs assemblies in aqueous solutions at different pH is obtained from DLS (Fig. 4.3). DLS results showed that a narrow size

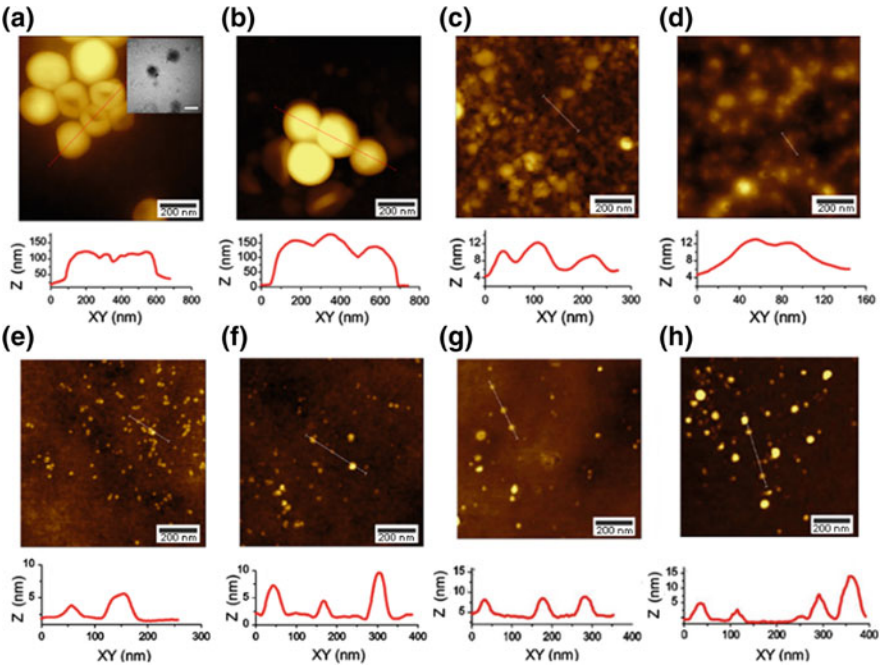

Fig. 4.2 AFM images of HBP-OILs $[C_{18}H_{37}]_{16}$-HBP-$([COO]^-[HMim]^+)_{16}$ (at pH 5.2 (**a**) and at pH 11.6 (**e**)), $[C_{18}H_{37}]_{16}$-HBP-$([COO]^-[HTri]^+)_{16}$ (at pH 5.2 (**b**) and at pH 11.6 (**f**)), $[C_{18}H_{37}]_{16}$-HBP-$([SO_3]^-[HMim]^+)_{16}$ (at pH 5.2 (**c**) and at pH 11.6 (**g**)) and $[C_{18}H_{37}]_{16}$-HBP-$([SO_3]^-[HTri]^+)_{16}$ (at pH 5.2 (**d**) and at pH 11.6 (**h**)) aqueous solutions deposited at pH 5.2 and pH 11.6 on silicon wafers and the corresponding height profiles along the lines. Scale bar is 200 nm. TEM image (insert on image (**a**)) of the HBP-OIL $[C_{18}H_{37}]_{16}$-HBP-$([COO]^-[HTri]^+)_{16}$ assemblies deposited from pH 5.2 solutions on carbon-formvar-coated copper grids. Reproduced with permission from [5], copyright (2016) American Chemical Society

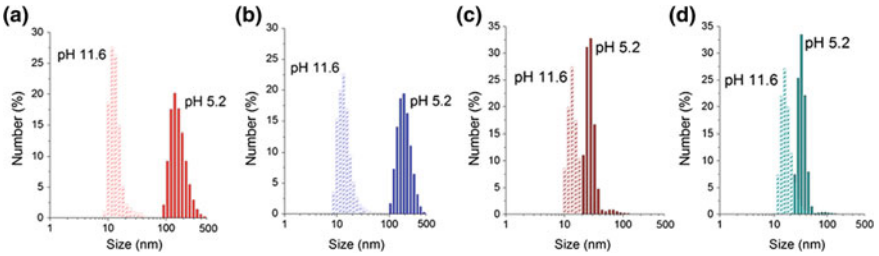

Fig. 4.3 Size distribution of micelles and their aggregates for HBP-OILs $[C_{18}H_{37}]_{16}$-HBP-$([COO]^-[HMim]^+)_{16}$ (**a**), $[C_{18}H_{37}]_{16}$-HBP-$([COO]^-[HTri]^+)_{16}$ (**b**) and $[C_{18}H_{37}]_{16}$-HBP-$([SO_3]^-[HMim]^+)_{16}$ (**c**), $[C_{18}H_{37}]_{16}$-HBP-$([SO_3]^-[HTri]^+)_{16}$ (**d**) in aqueous solution at different pH according to DLS data. Concentration of HBP-OILs is 0.2 mg/ml. Reproduced with permission from [5], copyright (2016) American Chemical Society

distribution (±4÷14 nm) is characteristic of the compounds with high ionicity of ionic groups (sulfonic HBP-OILs, Fig. 4.3c, d, Table 4.2) and high pH values of the medium (pH 11.6, Fig. 4.3a–d), while the assemblies formed by the carboxylate HBP-OILs in an acidic environment (pH 5.2) are characterized by a wide size distribution (±30÷60 nm) (Fig. 4.3a, b, Table 4.2).

Difference in the size distribution of the assemblies are also explained by the different extent of ionization of ionic groups; in particular, the wide distribution for carboxylic HBP-OILs at low pH is due to the low degree of ionization of ionic groups, which contributes to the micelle aggregation with large-sized supramolecular formation showing a corresponding statistical distribution.

Increasing the ionic strength of aqueous solutions via increase in NaCl concentration up to 0.1 M causes formation of micelles assemblies of 180–210 nm in size for carboxylate compounds $[C_{18}H_{37}]_{16}$-HBP-$([COO]^-[HMim]^+)_{16}$ and $[C_{18}H_{37}]_{16}$-HBP-$([COO]^-[HTri]^+)_{16}$ [5]. Further increase in the ionic strength leads to sedimentation. In case of sulfonate compounds ($[C_{18}H_{37}]_{16}$-HBP-$([SO_3]^-[HMim]^+)_{16}$ and $[C_{18}H_{37}]_{16}$-HBP-$([SO_3]^-[HTri]^+)_{16}$) the exceeding NaCl concentration of 0.6 M is accomplished by sedimentation [5]. The values of ζ-potentials for the compounds in aqueous solutions depends a little on pH and are in the range of −50 and −67 mV in accordance with electrophoretic light scattering (ELS) results (Table 4.2). The latter indicates high stability of micelles and their assemblies.

4.2.3 Assembly of Hyperbranched Oligomeric Ionic Liquids at Water/Air Interface

The values of the limiting mean molecular area (MMA) for the obtained HBP-OILs at water/air interface established by the LB method from the surface pressure-area isotherms are in the range of 13.8–18.6 nm^2/molecule (Fig. 4.4, Table 4.2).

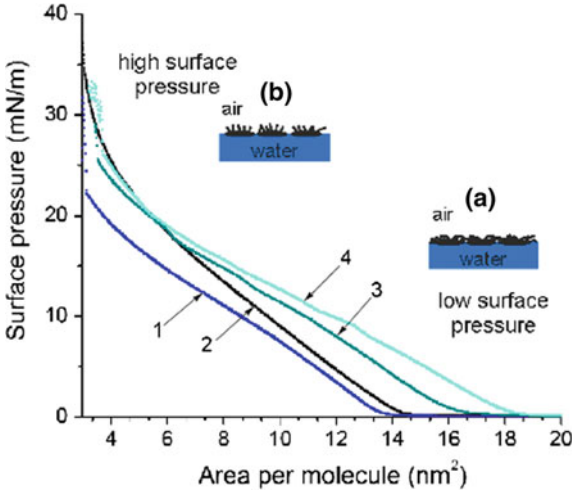

Fig. 4.4 Pressure-area isotherms for HBP-OILs $[C_{18}H_{37}]_{16}$-HBP-$([COO]^-[HMim]^+)_{16}$ (1), $[C_{18}H_{37}]_{16}$-HBP-$([COO]^-[HTri]^+)_{16}$ (2), $[C_{18}H_{37}]_{16}$-HBP-$([SO_3]^-[HMim]^+)_{16}$ (3) and $[C_{18}H_{37}]_{16}$-HBP-$([SO_3]^-[HTri]^+)_{16}$ (4) at water/air interface at 25 °C and sketches of molecular packing of monolayer at low (**a**) and high (**b**) surface pressures. Reproduced with permission from [5], copyright (2016) American Chemical Society

The sulfonate HBP-OILs are characterized by a larger MMA values compared to the carboxylate analogues due to more expanded conformation of sulfonate macromolecules as a result of their high ionicity. Also, the values of MMA for triazolium HBP-OILs are larger in comparison with those for imidazolium analogues due to solvation of imine group in triazolium ring by water molecules. In [4], we showed that when the number of ionic liquid groups in both imidazolium and triazolium carboxylate HBP-OILs are 24 and 16, the isotherms are characterized by the presence of the sections corresponding to gaseous and liquid states of Langmuir monolayers. Only when the content of ionic-liquid groups is minimum (8 groups) the isotherm sections corresponding to the solid state of the monolayer appeared.

The LB films of carboxylate imidazolium HBP-OILs with different content of ionic-liquid groups at a surface pressure in monolayers of 5 mN/m were obtained (Fig. 4.5) [4]. As the hydrophobic content is increased, the surface morphologies change from smooth featureless monolayers (compound $[C_{18}H_{37}]_8$-HBP-$([COO]^-[HMim]^+)_{24}$, Fig. 4.5a) to 2D surface micelles of 1–2 μm in diameter (compound $[C_{18}H_{37}]_{16}$-HBP-$([COO]^-[HMim]^+)_{16}$, Fig. 4.5b) and ultimately fractal-like aggregates (compound $[C_{18}H_{37}]_8$-HBP-$([COO]^-[HMim]^+)_{24}$, Fig. 4.5c). Surface aggregation will compromise interfacial stability.

4.3 Assembly of Linear and Hyperbranched Thermally Responsive Oligomeric and Polymeric Ionic Liquids in Aqueous Media and at the Water/Air Interface

The authors offered the direction of development of stimuli-responsive HBP-PILs, sensitive in terms of the structural organization of their supramolecular assemblies to

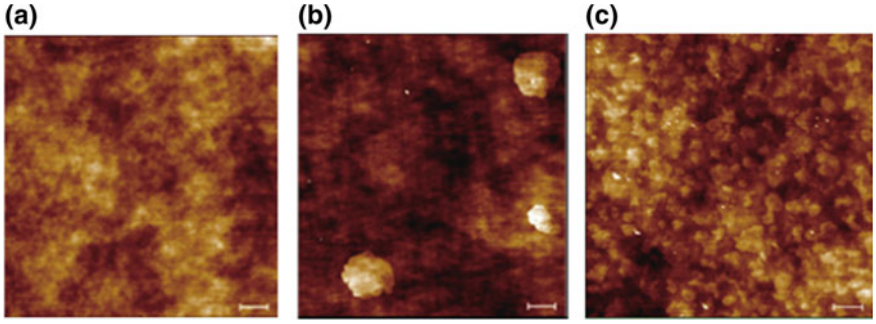

Fig. 4.5 AFM images of HBP-OILs $[C_{18}H_{37}]_8$-HBP-$([COO]^-[HMim]^+)_{24}$ (**a**), $[C_{18}H_{37}]_{16}$-HBP-$([COO]^-[HMim]^+)_{16}$ (**b**) and $[C_{18}H_{37}]_{24}$-HBP-$([COO]^-[HMim]^+)_8$ (**c**) LB films obtained at a surface pressure of 5 mN/m (scale bar 1 μm). Z-scale of all AFM images is 10 nm. Reproduced with permission from [4], copyright (2017) Chemical Society of Japan

temperature changes [29]. This direction was realized in the aspect of the synthesis of protic anionic HBP-PILs and their linear oligomeric analogs (OILs) with adjustable hydrophilic-hydrophobic balance, which contain thermally responsive macrocations showing LCST behavior.

These compounds are products of neutralization of linear and hyperbranched polyesters with terminal carboxyl groups by monoamine terminated poly(N-isopropylacrylamide) (PNIPAM) with $M_n = 2500$ g/mol. The synthesized compounds with ammonium thermally responsive PNIPAM macrocations are characterized by LCST at 33–35 °C [29]. This LCST behavior allows to adjust hydrophilic-hydrophobic properties of the compounds by temperature change and to control their self-organization in the aqueous solutions, at the water/air interface and in LB monomolecular ultrathin film. In addition, the hydrophilic-hydrophobic properties of these compounds were regulated by the content of ionic-liquid groups in their composition. It should be noted that the comparison of the self-assembling behavior of the synthesized HBP-PILs with their linear oligomeric analogs makes it possible to establish an understanding of the influence of the branched structure on their structuring process.

4.3.1 Synthesis of Thermally Responsive Linear and Hyperbranched Oligomeric and Polymeric Ionic Liquids

Poly(di(ethylene glycol) adipate) (PDA) $M_n = 800$ g/mol containing two terminal hydroxyl groups was used as an initial linear oligomer for synthesis of the linear OILs. This oligoester simulates chemical composition and amphiphilic properties of hyperbranched core of the HBP-PILs. A third-generation commercially available

HBP-OH Boltorn®H30, containing 32 terminal hydroxyl groups, was used as an initial oligomer for synthesis of the HBP-PILs. Introduction of terminal carboxyl groups into the composition of the above polyesters was carried out by reaction of acylation of the terminal hydroxyl groups with phthalic anhydride. The synthesized polycarboxylic acids were further used to produce the thermally responsive OILs and PILs by both partial (neutralization level 50%) and complete neutralization by the primary amino groups of PNIPAM (Fig. 4.6).

The abbreviation used to refer to the synthesized compounds reflects both the structure of macromolecules and the degree of neutralization of their terminal

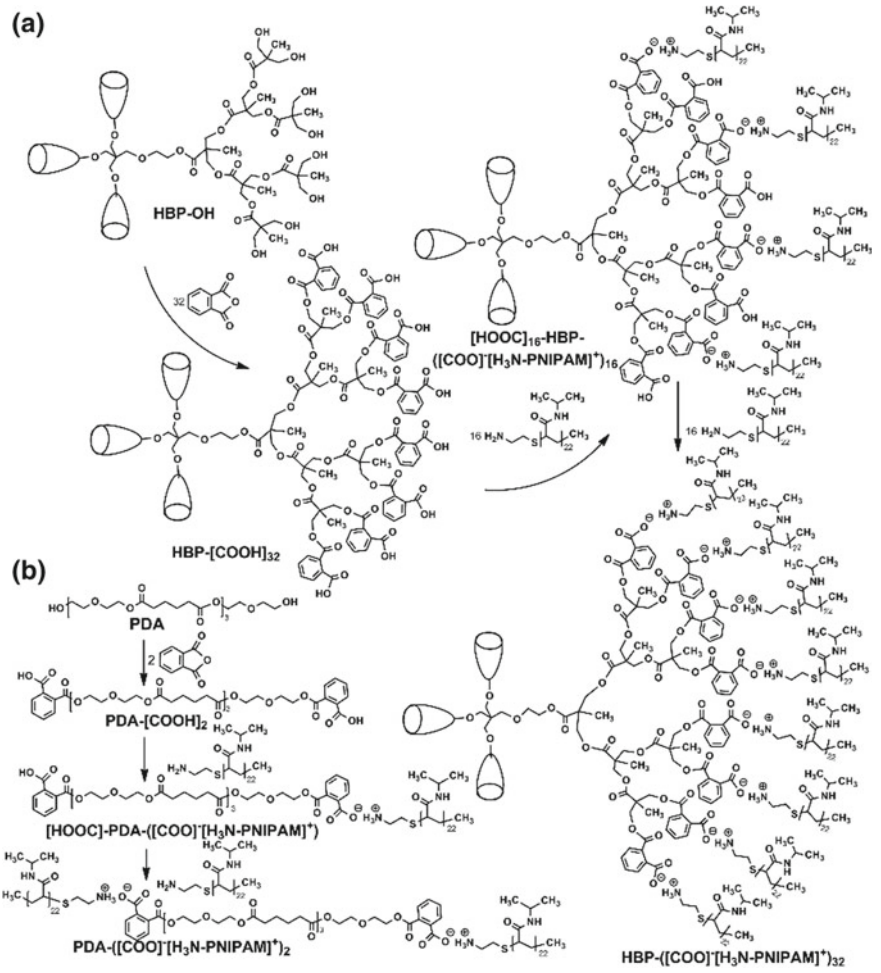

Fig. 4.6 Synthesis of the hyperbranched PILs (**a**) and the linear OILs (**b**) containing the thermally responsive PNIPAM macrocations. Reproduced with permission from [29], copyright (2018) American Chemical Society

carboxyl groups (Fig. 4.6). The linear oligomeric dicarboxylic acid and its partial (50%) and complete neutralized products are hereinafter referred to as PDA-$[COOH]_2$, [HOOC]-PDA-($[COO]^-[H_3N$-PNIPAM$]^+$) and PDA-($[COO]^-[H_3N$-PNIPAM$]^+)_2$ correspondingly and their hyperbranched analogues are referred to as HBP-$[COOH]_{32}$, $[HOOC]_{16}$-HBP-($[COO]^-[H_3N$-PNIPAM$]^+)_{16}$ and HBP-($[COO]^-[H_3N$-PNIPAM$]^+)_{32}$ respectively (Fig. 4.6). The compounds obtained were purified by reprecipitation from ethyl alcohol to diethyl ether.

The synthesized compounds are solid substances at room temperature, soluble in polar and insoluble in non-polar solvents. The solubility of these OILs and PILs in water is determined by the content of ionic groups in their composition: the increase in the content of ionic groups with PNIPAM fragments in the composition of the OILs and PILs favors their solubility in water at room temperature. Based on the content of carboxyl groups in the composition of initial oligomers, the degree of neutralization of carboxyl groups and the molecular weight (MW) of PNIPAM, the MW of synthesized linear OILs and hyperbranched PILs was determined (Table 4.3). The MW found and calculated on the basis of ideal compound formulas are close (Fig. 4.6).

According to DSC data the polycarboxylic acids, the OILs and the PILs are amorphous without any signs of crystallization which are characterized by high T_g (Table 4.3). T_g values of the synthesized compounds increase with increasing the content of the thermally responsive PNIPAM macrocation in their composition (Table 4.3), which is associated with the high rigidity of the PNIPAM macrocations (T_g values for PNIPAM are in the range of 110–140 °C) [30]). T_g values for the hyperbranched PILs is much higher than those for linear OILs. For example, T_g values of compounds $[HOOC]_{16}$-HBP-($[COO]^-[H_3N$-PNIPAM$]^+)_{16}$ and [HOOC]-

Table 4.3 MW characteristics and T_g values of the synthesized polycarboxylic acids, OILs and PILs

Sample	Peripheral groups (%)		MW (g/mol)		T_g (°C)
	–COOH	PNIPAM	Calculated	Found	
Linear architecture					
PDA-$[COOH]_2$	100	0	1096	1107	–
[HOOC]-PDA-($[COO]^-[H_3N$-PNIPAM$]^+$)	50	50	3596	3607	54
PDA-($[COO]^-[H_3N$-PNIPAM$]^+)_2$	3	97	6096	5957	77
Hyperbranched architecture					
HBP-$[COOH]_{32}$	100	0	8480	8471	34
$[HOOC]_{16}$-HBP-($[COO]^-[H_3N$-PNIPAM$]^+)_{16}$	51	49	48480	47671	94
HBP-($[COO]^-[H_3N$-PNIPAM$]^+)_{32}$	3	97	88480	86071	99

Adapted with permission from [29], copyright (2018) American Chemical Society

PDA-([COO]$^-$[H_3N-PNIPAM]$^+$) are 94 °C and 54 °C respectively (Table 4.3). The increase in T_g when the structure is changed from linear to hyperbranched is most likely related to an increase in the content of terminal functional groups and correspondingly rigid PNIPAM macrocations [3–7].

The turbidity experiment revealed that the LCST for the thermally responsive OILs and PILs is in the range of 33–35 °C (Table 4.4) and reduced by 1–3 °C compared to the values of typical PNIPAM containing OILs and PILs [31–33]. That is probably related to destabilization of salvating aqueous shell and salting out the PNIPAM fragments by ionic groups [34, 35]. Furthermore, the width of LCST transition for these compounds is within 1–2 °C which is narrower than usual LCST transition for PNIPAMs [5, 11, 29, 36, 37].

4.3.2 Assembly and Phase Transformations of Thermally Responsive Oligomeric and Polymeric Ionic Liquids in Aqueous Media

In aqueous media linear and hyperbranched compounds forms nanosized micellar assemblies with negative ζ-potential below LCST (Fig. 4.7, Table 4.4). According to DLS, the hydrodynamic diameter of micellar aggregates formed by the starting oligomeric polycarboxylic acids of linear and hyperbranched structure is 448 ± 55 nm (Fig. 4.7a) and 226 ± 109 nm, respectively (Fig. 4.7d). The size of the micellar aggregates from initial PDA-$[COOH]_2$ and HBP-$[COOH]_{32}$ is comparable with those for described in [38, 39] carboxylated hyperbranched polyesters. When the acids are neutralized by PNIPAM they form polydisperse assemblies with temperature dependent size (Fig. 4.7b, c, e, f, Table 4.4).

In this case, the size of such assemblies increases above LCST, which is associated with the transition of the PNIPAM macrocations into hydrophobic collapsed state, facilitating the coagulation of micelles and their aggregates [29, 40, 41]. It should be noted that the assemblies of compounds [HOOC]-PDA-([COO]$^-$[H_3N-PNIPAM]$^+$) and HBP-([COO]$^-$[H_3N-PNIPAM]$^+$)$_{32}$ are characterized by bimodal size distribution below (Fig. 4.7b) and above (Fig. 4.7f) LCST correspondingly, which can be related to ordering of macromolecules with various macrocation associations.

Completely neutralized linear oligomeric acid (compound PDA-([COO]$^-$[H_3N-PNIPAM]$^+$)$_2$) forms larger micellar aggregates (Fig. 7c, Table 4.4) than hyperbranched analogue (HBP-([COO]$^-$[H_3N-PNIPAM]$^+$)$_{32}$ does (Fig. 4.7f, Table 4.4). The decrease in size of such supramolecular structures is observed as a result of rise in content of PNIPAM component independently of the compounds architecture (Fig. 4.7a–f, Table 4.4). The size of micelles and micellar aggregates formed by linear OILs are in a good agreement with those for known thermally responsive polymers [42] and PILs [43] containing PNIPAM fragments.

Additional confirmation of spherical shape of OILs and PILs assemblies below LSCT comes from TEM images (Fig. 4.7g–l). TEM images evidence about larger

Table 4.4 Colloid-chemical characteristics of polycarboxylic acids, OILs and PILs assemblies

Sample	LCST (°C)	At 23 °C			At 38 °C		At 50 °C	
		D^{a}_{DLS} (nm)	D^{b}_{TEM} (nm)	ζ-pot. (mV)	D^{a}_{DLS} (nm)	ζ-pot. (mV)	D^{c}_{SEM} (μm)	ζ-pot. (mV)
Linear architecture								
PDA-$[COOH]_2$	–	448 ± 55	375 ± 40	−9.4 ± 4.6	520 ± 59	−15.0 ± 1.0	–	−22.1 ± 0.5
[HOOC]-PDA-($[COO]^-[H_3N$-PNIPAM$]^+$)	33.3 ± 0.1	10 ± 2, 380 ± 90	235 ± 60	−1.2 ± 0.2	2905 ± 210	−2.5 ± 0.2	4.2 ± 1.2	+8.9 ± 0.7
PDA-($[COO]^-[H_3N$-PNIPAM$]^+)_2$	34.0 ± 0.1	332 ± 74	170 ± 30	−2.6 ± 3.0	3299 ± 354	+1.4 ± 0.5	3.1 ± 0.8	+12.5 ± 1.0
Hyperbranched architecture								
HBP-$[COOH]_{32}$	–	226 ± 109	215 ± 60	−31.6 ± 1.6	220 ± 101	−35.9 ± 2.1	–	−32.7 ± 1.4
$[HOOC]_{16}$-HBP-($[COO]^-[H_3N$-PNIPAM$]^+)_{16}$	34.7 ± 0.1	253 ± 104	172 ± 57	−10.8 ± 2.7	2411 ± 306	−7.8 ± 1.9	7.2 ± 3.3	+1.9 ± 0.3
HBP-($[COO]^-[H_3N$-PNIPAM$]^+)_{32}$	34.3 ± 0.1	222 ± 60	70 ± 10	−10.2 ± 3.2	145 ± 30, 507 ± 119	−10.8 ± 1.7	1.3 ± 0.3	−1.1 ± 0.3

[a]Average size from DLS data; [b, c]Average size from TEM and SEM images, respectively
Adapted with permission from [29], copyright (2018) American Chemical Society

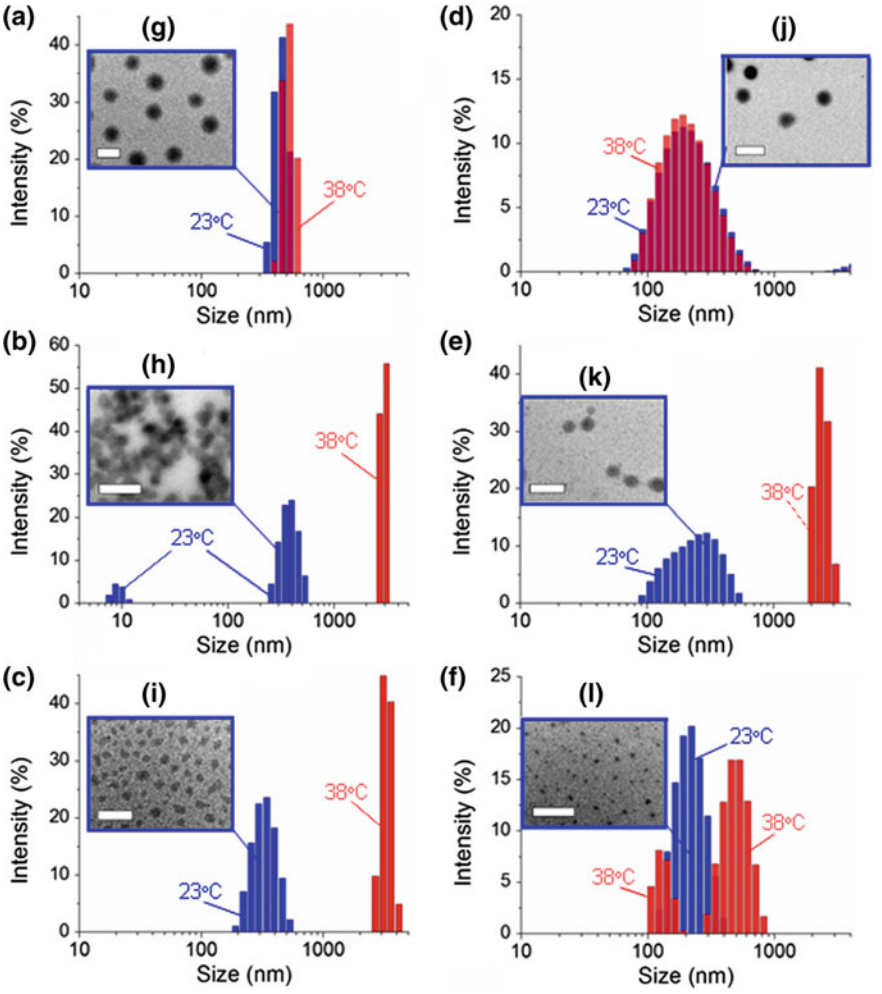

Fig. 4.7 Size distribution of micellar assemblies of linear compounds PDA-$[COOH]_2$ (**a**), [HOOC]-PDA-($[COO]^-[H_3N$-PNIPAM$]^+$) (**b**), PDA-($[COO]^-[H_3N$-PNIPAM$]^+)_2$ (**c**) and hyperbranched compounds HBP-$[COOH]_{32}$ (**d**), $[HOOC]_{16}$-HBP-($[COO]^-[H_3N$-PNIPAM$]^+)_{16}$ (**e**), and HBP-($[COO]^-[H_3N$-PNIPAM$]^+)_{32}$ (**f**) in aqueous media at 23 ± 0.2 °C and at 38 ± 0.2 °C according to DLS and corresponding TEM images (scale bar is 500 nm). Reproduced with permission from [29], copyright (2018) American Chemical Society

size of assemblies derived from compounds of linear architecture compared with those from hyperbranched analogues. (Fig. 4.7g–l, Table 4.4). Reducing size of the assemblies with rise in content of the thermally responsive component was also confirmed by TEM images (Fig. 4.7g–l, Table 4.4).

According to ELS data recorded at temperature below LCST, the initial hyperbranched oligomeric acid HBP-$[COOH]_{32}$ is characterized by the higher value of ζ-potential compared to the linear analogue PDA-$[COOH]_2$ (-31 ± 1.6 mV against -9.4 ± 4.6 mV correspondingly, Table 4.4) as a result of higher content of acidic groups [4]. Introduction of the PNIPAM component in composition of the oligomeric acids causes surface negative charge screening thereby significantly decreasing ζ-potential of assemblies independently of the compounds architecture (Table 4.4).

At the same time, the variation of the compound architecture (linear or hyperbranched) as well as the amount of PNIPAM macrocations plays a critical role in the design of multi-length scale micellar morphologies above LCST. When linear OILs [HOOC]-PDA-($[COO]^-[H_3N$-PNIPAM$]^+$) and PDA-($[COO]^-[H_3N$-PNIPAM$]^+)_2$ are deposited on silicon wafers above the LCST, they form micellar structures, namely submicron worm-like or network-like aggregates (Fig. 4.8a, b).

In contrast to the linear OILs, the branched PILs forms large vesicles (giant vesicles [44]) (Fig. 4.8c) or highly uniform, smaller spherical micelles above the LCST (Fig. 4.8d). Moreover, increasing the degree of neutralization up to 100% (compound

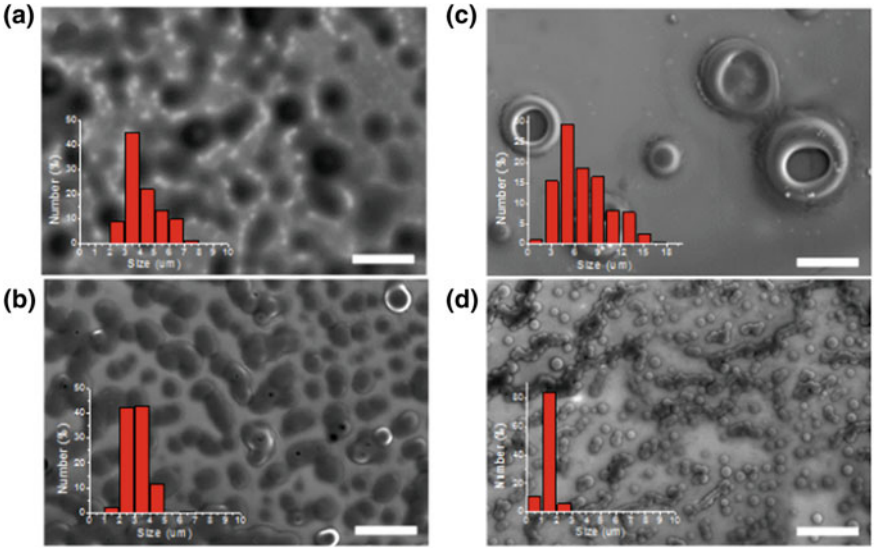

Fig. 4.8 SEM images of compounds [HOOC]-PDA-($[COO]^-[H_3N$-PNIPAM$]^+$) (**a**), PDA-($[COO]^-[H_3N$-PNIPAM$]^+)_2$ (**b**), $[HOOC]_{16}$-HBP-($[COO]^-[H_3N$-PNIPAM$]^+)_{16}$ (**c**) and HBP-($[COO]^-[H_3N$-PNIPAM$]^+)_{32}$ (**d**) deposited on silicon wafers from aqueous solutions at 50 ± 0.5 °C (scale bar is 20 μm) and corresponding size distributions of the assemblies (inserts). Reproduced with permission from [29], copyright (2018) American Chemical Society

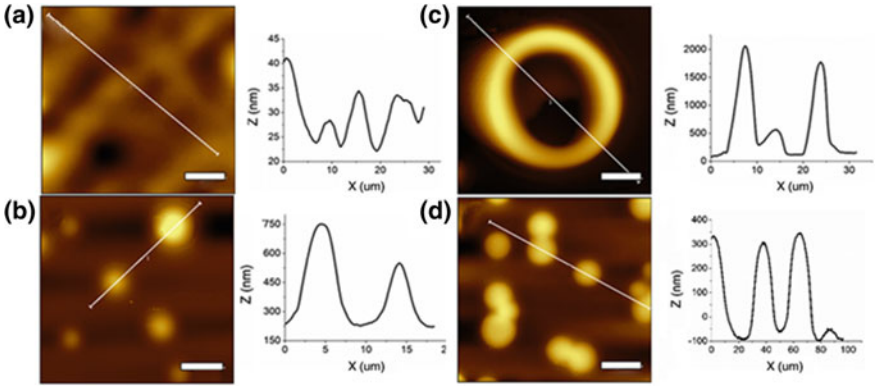

Fig. 4.9 AFM images of compounds [HOOC]-PDA-([COO]$^-$[H_3N-PNIPAM]$^+$) (**a**), PDA-([COO]$^-$[H_3N-PNIPAM]$^+$)$_2$ (**b**), [HOOC]$_{16}$-HBP-([COO]$^-$[H_3N-PNIPAM]$^+$)$_{16}$ (**c**) and HBP-([COO]$^-$[H_3N-PNIPAM]$^+$)$_{32}$ (**d**) deposited on silicon wafers from aqueous solutions at 50 ± 0.5 °C and corresponding height profiles along white lines (**e**–**h**). Scale bars are 5 μm for (**a**–**c**) and 2 μm for (**d**). Z scale is 70 nm (**a**), 800 nm (**b**), 2.3 μm (**c**), and 500 nm (**d**). Reproduced with permission from [29], copyright (2018) American Chemical Society

HBP-([COO]$^-$[H_3N-PNIPAM]$^+$)$_{32}$) leads to formation of chain-like aggregates of much smaller and highly uniform spherical micelles without fusion (Fig. 4.8d).

AFM images of dried micellar assemblies above the LCST confirm that [HOOC]-PDA-([COO]$^-$[H_3N-PNIPAM]$^+$) (Fig. 4.9a) and PDA-([COO]$^-$[H_3N-PNIPAM]$^+$)$_2$ (Fig. 4.9b) OILs form submicron aggregates with network-like and spherical morphology. On the other hand, HBP-PILs [HOOC]$_{16}$-HBP-([COO]$^-$[H_3N-PNIPAM]$^+$)$_{16}$ (Fig. 4.9c) and HBP-([COO]$^-$[H_3N-PNIPAM]$^+$)$_{32}$ (Fig. 4.9d) are assembled into giant vesicles and smaller spherical aggregates that correlates with SEM data (Fig. 4.8c and d correspondingly).

Furthermore, the temperature-triggered transformation of PNIPAM macrocations of the OILs and HBP-PILs at temperature above LCST shifts the ζ-potential of the assemblies from about −3 mV to +13 mV for the linear compounds and from −10 mV to ~0 mV for the hyperbranched compounds at maximum content of thermally responsive macrocations (Table 4.4). This shift indicates folding the PNIPAM fragments which screen the surface ionic groups of the assemblies that favors the compound aggregation above the LCST [5].

4.3.3 Assembly of Thermally Responsive Oligomeric and Polymeric Ionic Liquids at Water/Air Interface

The features of self-organization of the initial polycarboxylic acids (PDA-[COOH]$_2$, HBP-[COOH]$_{32}$), linear OILs ([HOOC]-PDA-([COO]$^-$[H_3N-PNIPAM]$^+$) and PDA-([COO]$^-$[H_3N-PNIPAM]$^+$)$_2$), and hyperbranched PILs ([HOOC]$_{16}$-HBP-

($[COO]^-[H_3N\text{-}PNIPAM]^+)_{16}$ and HBP-($[COO]^-[H_3N\text{-}PNIPAM]^+)_{32}$) in Langmuir monolayers at water/air interface and in LB films on silicon wafers were studied. The effect of the architecture and content of thermally responsive PNIPAM macrocations on the assembly at different temperatures was shown.

The pressure-area isotherms were found for all samples (PDA-$[COOH]_2$, [HOOC]-PDA-($[COO]^-[H_3N\text{-}PNIPAM]^+$), PDA-($[COO]^-[H_3N\text{-}PNIPAM]^+)_2$, HBP-$[COOH]_{32}$, $[HOOC]_{16}$-HBP-($[COO]^-[H_3N\text{-}PNIPAM]^+)_{16}$ and HBP-($[COO]^-[H_3N\text{-}PNIPAM]^+)_{32}$) at both 23 and at 37 °C using the LB trough (Fig. 4.10). The synthesized compounds form stable Langmuir monolayers at water/air interface and their compression isotherms are characterized by the presence of the sections corresponding to gaseous, liquid and solid state of monolayers [18, 19].

When heated, PNIPAM macrocations demonstrates LCST behavior while the oligoester component in aqueous media shows no temperature dependence [29, 34]. Therefore, no change in the isotherms between 23 and 37 °C for the oligomeric acids (samples PDA-$[COOH]_2$ and HBP-$[COOH]_{32}$) was expected (Fig. 4.10). In contrast to initial acids, there is a substantial difference (including MMA, see below Table 4.5) between the isotherms of the compounds containing PNIPAM macrocations (samples [HOOC]-PDA-($[COO]^-[H_3N\text{-}PNIPAM]^+$), PDA-($[COO]^-[H_3N\text{-}PNIPAM]^+)_2$, $[HOOC]_{16}$-HBP-($[COO]^-[H_3N\text{-}PNIPAM]^+)_{16}$ and HBP-($[COO]^-[H_3N\text{-}PNIPAM]^+)_{32}$) at 23 and 37 °C (Fig. 4.10). The profiles of the obtained curves indicate an increase in the critical pressure in monolayers, leading to their collapse, with increasing the content of ionic groups in

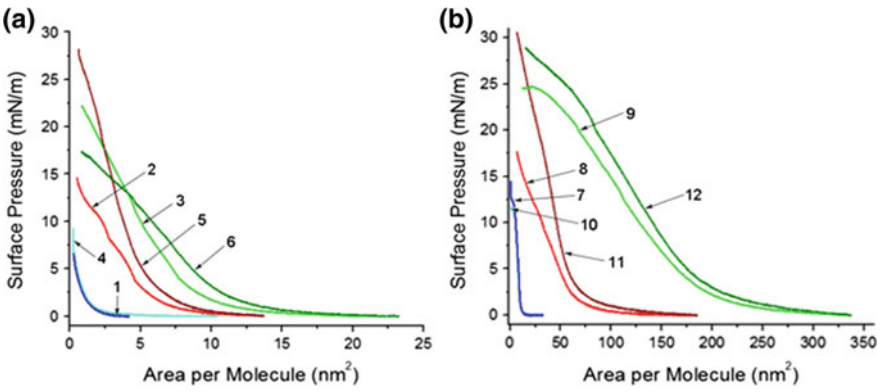

Fig. 4.10 Pressure-area isotherms for the polycarboxylic acids, the OILs and the HBP-PILs monolayers at water/air interface: **a** for linear compound PDA-$[COOH]_2$ (at room temperature (1) and at 37.9 °C (4)), [HOOC]-PDA-($[COO]^-[H_3N\text{-}PNIPAM]^+$) (at room temperature (2) and at 37.9 °C (5)) and PDA-($[COO]^-[H_3N\text{-}PNIPAM]^+)_2$ (at room temperature (3) and at 37.9 °C (6)); **b** for hyperbranched compound HBP-$[COOH]_{32}$ (at room temperature (7) and at 37.9 °C (10)), $[HOOC]_{16}$-HBP-($[COO]^-[H_3N\text{-}PNIPAM]^+)_{16}$ (at room temperature (8) and at 37.9 °C (11)) and HBP-($[COO]^-[H_3N\text{-}PNIPAM]^+)_{32}$ (at room temperature (9) and at 37.9 °C (12))

Table 4.5 Limiting MMA of the synthesized polycarboxylic acids, OILs and PILs at water/air interface and roughness of LB films based on them at room temperature and at 37 °C

Sample	MMA (nm^2/molecule)		Roughness[a] (nm)	
	At 23 °C	At 37 °C	At 23 °C	At 37 °C
Linear architecture				
PDA-$[COOH]_2$	1.4	0.9	1.13	1.32
[HOOC]-PDA-($[COO]^-[H_3N$-PNIPAM$]^+$)	6.4	5.3	1.35	1.29
PDA-($[COO]^-[H_3N$-PNIPAM$]^+)_2$	8.9	11.4	1.34	1.11
Hyperbranched arcitecture				
HBP-$[COOH]_{32}$	12.1	10.6	1.14	1.15
$[HOOC]_{16}$-HBP-($[COO]^-[H_3N$-PNIPAM$]^+)_{16}$	68.7	66.7	1.27	1.15
HBP-($[COO]^-[H_3N$-PNIPAM$]^+)_{32}$	191.2	204.4	1.43	1.23

[a] 10×10 μm surface area

the composition of the compounds, as well as temperature exceeding the LCST in the presence of thermally responsive component.

Using the pressure-area isotherms (Fig. 4.10), the limiting MMA was found for all samples (Table 4.5). The MMA values for the hyperbranched samples (HBP-$[COOH]_{32}$, $[HOOC]_{16}$-HBP-($[COO]^-[H_3N$-PNIPAM$]^+)_{16}$ and HBP-($[COO]^-[H_3N$-PNIPAM$]^+)_{32}$) are much higher than those for the linear analogues (PDA-$[COOH]_2$, [HOOC]-PDA-($[COO]^-[H_3N$-PNIPAM$]^+$) and PDA-($[COO]^-[H_3N$-PNIPAM$]^+)_2$) below LCST. In addition, a large increase in MMA can be seen with increasing PNIPAM content for all compounds studied here. For example, the MMA values of linear and hyperbranched compounds increase by ~270% and by ~30% when PNIPAM content increases from 50 to 100% (Table 4.5).

The decrease in limiting MMA for the initial oligomeric acids (by 36% and 12% for samples PDA-$[COOH]_2$ and HBP-$[COOH]_{32}$ correspondingly (Table 4.5)) can be promoted by slight rearrangement and better molecular packing of the hydrophobic parts of the molecules due to the higher energy from the increased temperature [45]. At the same time, the MMA values for the compounds with partially neutralized carboxylic groups (samples [HOOC]-PDA-($[COO]^-[H_3N$-PNIPAM$]^+$) and $[HOOC]_{16}$-HBP-($[COO]^-[H_3N$-PNIPAM$]^+)_{16}$) decreased less (by 17% and 3% correspondingly) in comparison with initial oligomeric acids as the temperature increased (Table 4.5). This trend of MMA of linear and hyperbranched compounds can be attributed to the rearrangement of the PNIPAM component as it changed from a swollen hydrophilic state below LCST to a condensed hydrophobic state above LCST. If the condensed hydrophobic PNIPAM fragments positioned themselves out of the water and above the oligoester hydrophobic component, only a small decrease in limiting MMA would be seen (Fig. 4.11).

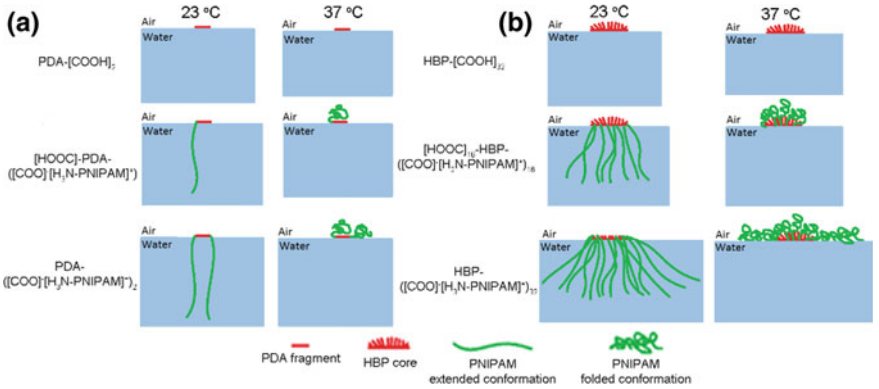

Fig. 4.11 Conformational behavior of the synthesized linear (**a**) and hyperbranched (**b**) polycarboxylic acids, OILs and PILs at water/air interface at both room temperature and 37 °C

Unlike the compounds with partially neutralized carboxylic groups ([HOOC]-PDA-([COO]$^-$[H_3N-PNIPAM]$^+$) and [HOOC]$_{16}$-HBP-([COO]$^-$[H_3N-PNIPAM]$^+$)$_{16}$) the limiting MMA for the fully neutralized compounds (PDA-([COO]$^-$[H_3N-PNIPAM]$^+$)$_2$ (Fig. 4.10a) and HBP-([COO]$^-$[H_3N-PNIPAM]$^+$)$_{32}$ (Fig. 4.10b) increased by 28% and 7% correspondingly as the temperature increased (Table 4.5). Because the size of hydrophobic oligoester component is limited, only a limited amount of condensed PNIPAM segments can position themselves directly above the oligoester hydrophobic component (Fig. 4.11), and the rest of the PNIPAM groups spread on the water surface. Therefore, the limiting MMA would increase if too many PNIPAM groups are added [46, 47].

The AFM images of LB films formed by initial oligomeric acids PDA-[COOH]$_2$ and HBP-[COOH]$_{32}$ at 23 and 37 °C at surface pressure of 5 mN/m which corresponds to solid state of Langmuir monolayer (Fig. 4.10) show no temperature dependence and no visible micelles (Fig. 4.12). The explanation for this result can be that these compounds do not have sufficient hydrophobic parts to form spheres with the correct proportions of hydrophobic centers and hydrophilic surfaces. No micelles were observed under the same conditions for any of the linear OILs.

In contrast to linear OILs, branched PILs (samples HBP-PILs [HOOC]16-HBP-([COO]-[H3N-PNIPAM]+)$_{16}$ and HBP-([COO]-[H_3N-PNIPAM]+)$_{32}$) form aggregates of 1–2 μm in size above LCST (Fig. 4.12b). We suggest that the aggregation of HBP-ILs can be explained by increasing hydrophobicity of the compounds as a result of PNIPAM folding [4, 5].

In addition, we found a slight increase in (~10%) surface microroughness (determined on area of 10 × 10 μm) of the obtained LB films with increasing PNIPAM content for HBP-ILs (Table 4.5). There is also a more significant decrease in the surface roughness of the films by 5–20% as temperature increased (Table 4.5). Such behavior of the compounds indicates the existence of spatial hindrances at temperatures below LCST caused by bulk PNIPAM substituents in the expanded state, which

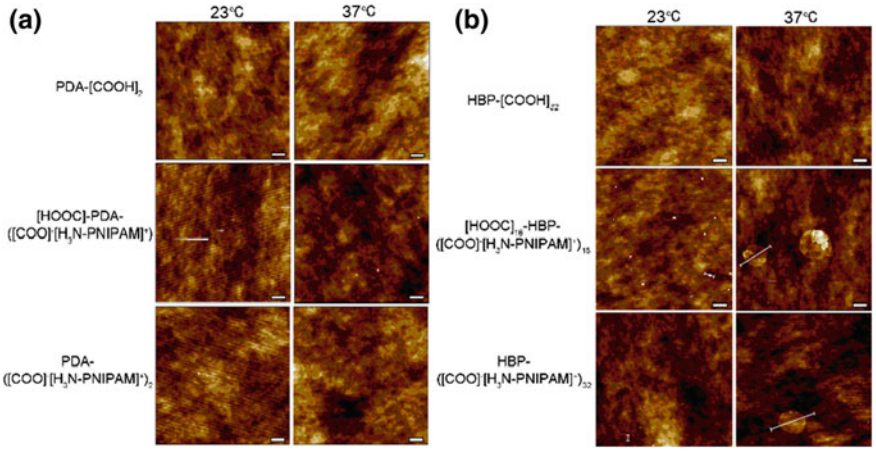

Fig. 4.12 AFM images of LB films formed by the polycarboxylic acids, the OILs and the PILs of linear (**a**) and hyperbranched (**b**) architecture at a surface pressure of 5 mN/m at 23 and 37 °C (scale bar is 1 μm)

prevents a dense packing of macromolecules. This results in rougher surface of the films. On the other hand, at temperatures above LCST the collapsed state causes a decrease in spatial hindrances and favors the formation of smoother films.

Overall, we demonstrated the variation of the content of ionic groups with PNIPAM macrocations in the composition of the synthesized linear and hyperbranched compounds allows us to obtain the smooth (microroughness <1.5 nm) ultrathin films with various morphologies which are promising for use as polyelectrolyte coatings with an adjustable thermally responsive structure in microelectronics, sensors, catalytic systems, and surface-orientation layers.

4.4 Conclusions

In this study, we summarize our recent efforts on synthesis and aqueous assembly of series of amphiphilic anionic protic oligomeric and polymeric ionic liquids based on hyperbranched polyfunctional acids core with various neutralization degrees of the peripheral carboxyl or sulfonic acid groups with N-methylimidazole (Im) and 1,2,4-1H-triazole (Tr) or monoamine-terminated poly(N-isopropylacrylamide)s, and their linear analogues. We find that introduction of long-chain aliphatic tails into the composition of the synthesized compounds enables them to form a crystalline phase. Moreover, these amphiphilic oligomeric and polymeric ionic liquids show unique chemically- and thermally-induced self-assembling behaviour with morphologies tuned by a chemical architecture, namely the content of hydrophilic ionic groups or hydrophobic long-chain aliphatic tails and linear or hyperbranched architecture of initial polycarboxylic acids.

The assembly of these compounds into core–corona micelles in aqueous media in a wide range of pH and ionic conditions was established. The introduction of long hydrophobic aliphatic tails to starting hydrophobic hyperbranched core influences more significantly on the size of micellar assemblies than the introduction of ionic groups does. Regulation of HBP-OILs amphiphilicity can be realized by varying the extent of ionization of terminal groups by changing pH or ionic strength. A more loose conformation of macromolecules at water/air interface is characteristic for the sulfonate HBP-OILs that is due to their higher ionicity compared to carboxylate analogues.

As the content of aliphatic long-chain hydrophobic tails is increased, the surface morphology of LB films of carboxylate imidazolium HBP-OILs is varied from smooth featureless monolayers to 2D surface micelles and ultimately fractal-like aggregates.

The thermally responsive HBP-PILs were obtained by neutralization of terminal carboxyl groups of aliphatic polyester core by monoamine-terminated PNIPAM (50 and 100%). These compounds possessed LCST behavior with a narrow LCST window and are amorphous in condensed state.

The OILs and PILs self-assemble into spherical micelles and their aggregates of different morphologies that is determined by their chemical structure. When temperature is higher than LCST the formation of spherical micelles, network-like aggregates and large vesicles is observed. In opposite to initial cores prone to form spherical domains the thermally responsive compounds are able to self-assemble into elongated unimolecular nanodomain. Increasing PNIPAN content in the composition of the compounds and exceeding LCST contribute to the increase in the area occupied by macromolecules at water/air interface. It was shown that the formation of large micellar aggregates of few μm in LB films was observed only for the HBP-PILs and at temperature above LCST.

Such a variation of chemical architecture of ionic compounds promotes multiscale tuning of the morphology of their assemblies which are not accessible to low molar mass ionic liquids. This novel morphological tunability can open a new pathway to compounds and materials with unique transport characteristics for ion-conducting media for different electrochemical devices, drug-delivery systems, tissue engineering, membrane and sensor technologies, catalytic systems, functional ultrathin coatings for optics, microelectronics and surface-orientation layers.

Acknowledgements This study was financially supported by the National Science Foundation DMR 150523 project (USA), and by program of fundamental studies of the NAS of Ukraine "Novel Functional Substances and Materials of Chemical Production" (project N 16-18).

References

1. T.E. Long, Y.A. Elabd, J. Yuan, Ionic liquids in polymer design. Macromol. Rapid Commun. **37**(14), 1105 (2016). https://doi.org/10.1002/marc.201600255
2. D. Mecerreyes, Polymeric ionic liquids: broadening the properties and applications of polyelectrolytes. Prog. Polym. Sci. **36**(12), 1629–1648 (2011). https://doi.org/10.1016/j.progpolymsci.2011.05.007
3. W. Xu, P.A. Ledin, V.V. Shevchenko, V.V. Tsukruk, Architecture, assembly, and emerging applications of branched functional polyelectrolytes and poly(ionic liquid)s. ACS Appl. Mater. Interfaces. **7**(23), 12570–12596 (2015). https://doi.org/10.1021/acsami.5b01833
4. V.F. Korolovych, A.J. Erwin, A. Stryutsky, E.K. Mikan, V.V. Shevchenko, V.V. Tsukruk, Self-assembly of hyperbranched protic poly(ionic liquid)s with variable peripheral amphiphilicity. Bull. Chem. Soc. Jpn **90**(8), 919–923 (2017). https://doi.org/10.1246/bcsj.20170121
5. V.F. Korolovych, P.A. Ledin, A. Stryutsky, V.V. Shevchenko, O. Sobko, W. Xu, L.A. Bulavin, V.V. Tsukruk, Assembly of amphiphilic hyperbranched polymeric ionic liquids in aqueous media at different pH and ionic strength. Macromolecules **49**(22), 8697–8710 (2016). https://doi.org/10.1021/acs.macromol.6b01562
6. V.V. Shevchenko, A.V. Stryutsky, N.S. Klymenko, M.A. Gumenna, A.A. Fomenko, V.N. Bliznyuk, V.V. Trachevsky, V.V. Davydenko, V.V. Tsukruk, Protic and aprotic anionic oligomeric ionic liquids. Polymer **55**(16), 3349–3359 (2014). https://doi.org/10.1016/j.polymer.2014.04.020
7. V.V. Shevchenko, A.V. Stryutsky, O.A. Sobko, V.F. Korolovich, N.S. Klimenko, M.A. Gumennaya, V.V. Klepko, Y.V. Yakovlev, V.V. Davidenko, Amphiphilic protic anionic oligomeric ionic liquids of hyperbranched structure. Polymer Sci. B **59**(4), 379–391 (2017). https://doi.org/10.1134/S1560090417040108
8. A.S. Shaplov, R. Marcilla, D. Mecerreyes, Recent advances in innovative polymer electrolytes based on poly(ionic liquid)s. Electrochim. Acta **175**, 18–34 (2015). https://doi.org/10.1016/j.electacta.2015.03.038
9. S. Prescher, F. Polzer, Y. Yang, M. Siebenbürger, M. Ballauff, J. Yuan, Polyelectrolyte as solvent and reaction medium. J. Am. Chem. Soc. **136**(1), 12–15 (2014). https://doi.org/10.1021/ja409395y
10. S. Peleshanko, V.V. Tsukruk, The architectures and surface behavior of highly branched molecules. Prog. Polym. Sci. **33**(5), 523–580 (2008). https://doi.org/10.1016/j.progpolymsci.2008.01.003
11. D. Wang, Y. Jin, X. Zhu, D. Yan, Synthesis and applications of stimuli-responsive hyperbranched polymers. Prog. Polym. Sci. **64**, 114–153 (2017). https://doi.org/10.1016/j.progpolymsci.2016.09.005
12. V.V. Tsukruk, Dendritic macromolecules at interfaces. Adv. Mater. **10**(3), 253–257 (1998). https://doi.org/10.1002/(SICI)1521-4095(199802)10:3%3c253:AID-ADMA253%3e3.0.CO;2-E
13. V.V. Tsukruk, F. Rinderspacher, V.N. Bliznyuk, Self-assembled multilayer films from dendrimers. Langmuir **13**(8), 2171–2176 (1997). https://doi.org/10.1021/la960603h
14. X. Zhai, S. Peleshanko, N.S. Klimenko, K.L. Genson, D. Vaknin, M.Y. Vortman, V.V. Shevchenko, V.V. Tsukruk, Amphiphilic dendritic molecules: hyperbranched polyesters with alkyl-terminated branches. Macromolecules **36**(9), 3101–3110 (2003). https://doi.org/10.1021/ma021383j
15. J. Cho, K. Char, J.-D. Hong, K.-B. Lee, Fabrication of highly ordered multilayer films using a spin self-assembly method. Adv. Mater. **13**(14), 1076–1078 (2001). https://doi.org/10.1002/1521-4095(200107)13:14%3c1076:AID-ADMA1076%3e3.0.CO;2-M
16. P. Bertrand, A. Jonas, A. Laschewsky, R. Legras, Ultrathin polymer coatings by complexation of polyelectrolytes at interfaces: suitable materials, structure and properties. Macromol. Rapid Commun. **21**(7), 319–348 (2000). https://doi.org/10.1002/(SICI)1521-3927(20000401)21:7%3c319:AID-MARC319%3e3.0.CO;2-7

17. J.A. Zasadzinski, R. Viswanathan, L. Madsen, J. Garnaes, D.K. Schwartz, Langmuir-Blodgett films. Science **263**(5154), 1726–1733 (1994)
18. S.A. Hussain, S. Deb, D. Bhattacharjee, Langmuir-Blodgett technique a unique tool for fabrication of ultrathin organic films. J. Environ. Sci. Res. **4**, 25–33 (2005)
19. V.V. Tsukruk, Assembly of supramolecular polymers in ultrathin films. Prog. Polym. Sci. **22**(2), 247–311 (1997). https://doi.org/10.1016/S0079-6700(96)00005-6
20. A. Kausar, Survey on Langmuir–Blodgett films of polymer and polymeric composite. *Polymer-Plastics Technology and Engineering*, vol. 56, no. 9, pp. 932–945. https://doi.org/10.1080/03602559.2016.1247282
21. V. Shembekar, A. Contractor, S. Major, S. Talwar, Photoisomerization of amphiphilic azobenzene derivatives in Langmuir Blodgett films prepared as polyion complexes, using ionic polymers. Thin Solid Films **510**, 297–304 (2006). https://doi.org/10.1016/j.tsf.2005.12.210
22. T. Yoshimi, M. Moriyama, S. Ujiie, Orientational behavior of ionic liquid crystal polymers and their nonionic family. Mol. Cryst. Liq. Cryst. **511**(1), 319/[1789]–1326/[1796]. https://doi.org/10.1080/15421400903054428
23. T. Yoshimi, S. Ujiie, Self-assembly and liquid crystalline properties of ionic polymers and their nonionic family. Macromol. Symp. **242**(1), 290–294 (2006). https://doi.org/10.1002/masy.200651040
24. A. Nayak, K.A. Suresh, Conductivity of Langmuir-Blodgett films of a disk-shaped liquid-crystalline molecule-DNA complex studied by current-sensing atomic force microscopy. Phys. Rev. E: Stat. Nonlin. Soft Matter Phys. **78**(2 Pt 1), 021606 (2008). https://doi.org/10.1103/PhysRevE.78.021606
25. A.J. Erwin, W. Xu, H. He, K. Matyjaszewski, V.V. Tsukruk, Linear and star poly(ionic liquid) assemblies: surface monolayers and multilayers. Langmuir **33**(13), 3187–3199 (2017). https://doi.org/10.1021/acs.langmuir.6b04622
26. V. Pérez-Gregorio, I. Giner, M.C. López, I. Gascón, E. Cavero, R. Giménez, Influence of the liquid crystal behaviour on the Langmuir and Langmuir-Blodgett film supramolecular architecture of an ionic liquid crystal. J. Colloid Interface Sci. **375**, 94–101 (2012). https://doi.org/10.1016/j.jcis.2012.02.049
27. V. Shevchenko, A.V. Stryutsky, O.O. Sobko, N.S. Klimenko, M.A. Gumenna, Peculiarities of self-organization of amphiphilic oligomeric protic ionic liquids of hyperbranched structure with the formation of various hierarchical nanostructures. Theor. Exp. Chem. **54** (2018). https://doi.org/10.1007/s11237-018-9555-9
28. U.A. Rana, I. Shakir, R. Vijayraghavan, D.R. MacFarlane, M. Watanabe, M. Forsyth, Proton transport in acid containing choline dihydrogen phosphate membranes for fuel cell. Electrochim. Acta **111**, 41–48 (2013). https://doi.org/10.1016/j.electacta.2013.07.144
29. V.F. Korolovych, A. Erwin, A. Stryutsky, H. Lee, W.T. Heller, V.V. Shevchenko, L.A. Bulavin, V.V. Tsukruk, Thermally responsive hyperbranched poly(ionic liquid)s: assembly and phase transformations. Macromolecules **51**(13), 4923–4937 (2018). https://doi.org/10.1021/acs.macromol.8b00845
30. E. Lizundia, E. Meaurio, J.M. Laza, J.L. Vilas, L.M. León Isidro, Study of the chain microstructure effects on the resulting thermal properties of poly(L-lactide)/poly(N-isopropylacrylamide) biomedical materials. Mater. Sci. Eng., C **50**, 97–106 (2015). https://doi.org/10.1016/j.msec.2015.01.097
31. J.-W. Seo, J.-Y. Hwang, U.S. Shin, Ionic liquid-doped and p-NIPAAm-based copolymer (p-NIBIm): extraordinary drug-entrapping and -releasing behaviors at 38–42 °C. RSC Adv. **4**(51), 26738–26747 (2014). https://doi.org/10.1039/C4RA03736G
32. J. Illescas, M. Casu, V. Alzari, D. Nuvoli, M.A. Scorciapino, R. Sanna, V. Sanna, A. Mariani, Poly(ionic liquid)s derived from 3-octyl-1-vinylimidazolium bromide and N-isopropylacrylamide with tunable properties. J. Polym. Sci. Part A Polym. Chem. **52**(24), 3521–3532 (2014). https://doi.org/10.1002/pola.27418
33. E. Karjalainen, N. Chenna, P. Laurinmäki, S.J. Butcher, H. Tenhu, Diblock copolymers consisting of a polymerized ionic liquid and poly(N-isopropylacrylamide). Effects of PNIPAM block length and counter ion on self-assembling and thermal properties. Polym. Chem. **4**(4), 1014–1024 (2013). https://doi.org/10.1039/c2py20815f

34. K. Jain, R. Vedarajan, M. Watanabe, M. Ishikiriyama, N. Matsumi, Tunable LCST behavior of poly(N-isopropylacrylamide/ionic liquid) copolymers. Polym. Chem. **6**(38), 6819–6825 (2015). https://doi.org/10.1039/C5PY00998G
35. S. Jung, K.I. MacConaghy, J.L. Kaar, M.P. Stoykovich, Enhanced optical sensitivity in thermoresponsive photonic crystal hydrogels by operating near the phase transition. ACS Appl. Mater. Interfaces **9**(33), 27927–27935 (2017). https://doi.org/10.1021/acsami.7b07179
36. Y. Men, H. Schlaad, J. Yuan, Cationic poly(ionic liquid) with tunable lower critical solution temperature-type phase transition. ACS Macro. Lett. **2**(5), 456–459 (2013). https://doi.org/10.1021/mz400155r
37. Y. Kohno, S. Saita, Y. Men, J. Yuan, H. Ohno, Thermoresponsive polyelectrolytes derived from ionic liquids. Polym. Chem. **6**(12), 2163–2178 (2015). https://doi.org/10.1039/C4PY01665C
38. Y. Zhou, W. Huang, J. Liu, X. Zhu, D. Yan, Self-assembly of hyperbranched polymers and its biomedical applications. Adv. Mater. **22**(41), 4567–4590 (2010). https://doi.org/10.1002/adma.201000369
39. L. Liu, L. Rui, Y. Gao, W. Zhang, Self-assembly and disassembly of a redox-responsive ferrocene-containing amphiphilic block copolymer for controlled release. Polym. Chem. **6**(10), 1817–1829 (2015). https://doi.org/10.1039/C4PY01289E
40. G. Li, S. Song, L. Guo, S. Ma, Self-assembly of thermo-and pH-responsive poly (acrylic acid)-b-poly (N-isopropylacrylamide) micelles for drug delivery. J. Polym. Sci. Part A Polym. Chem. **46**(15), 5028–5035 (2008)
41. G. Li, L. Shi, Y. An, W. Zhang, R. Ma, Double-responsive core–shell–corona micelles from self-assembly of diblock copolymer of poly(t-butyl acrylate-co-acrylic acid)-b-poly(N-isopropylacrylamide). Polymer **47**(13), 4581–4587 (2006). https://doi.org/10.1016/j.polymer.2006.04.041
42. J. Guo, Y. Zhou, L. Qiu, C. Yuan, F. Yan, Self-assembly of amphiphilic random co-poly(ionic liquid)s: the effect of anions, molecular weight, and molecular weight distribution. Polym. Chem. **4**(14), 4004–4009 (2013). https://doi.org/10.1039/C3PY00460K
43. M. Sahn, T. Yildirim, M. Dirauf, C. Weber, P. Sungur, S. Hoeppener, U.S. Schubert, LCST behavior of symmetrical PNiPAm-b-PEtOx-b-PNiPAm triblock copolymers. Macromolecules **49**(19), 7257–7267 (2016). https://doi.org/10.1021/acs.macromol.6b01371
44. Y. Zhou, D. Yan, Supramolecular self-assembly of giant polymer vesicles with controlled sizes. Angew. Chem. Int. Ed. **43**(37), 4896–4899 (2004). https://doi.org/10.1002/anie.200460325
45. M. Jaremko, Ł. Jaremko, H.-Y. Kim, M.-K. Cho, C.D. Schwieters, K. Giller, S. Becker, M. Zweckstetter, Cold denaturation of a protein dimer monitored at atomic resolution. Nat. Chem. Biol. **9**(4), 264–270 (2013). https://doi.org/10.1038/nchembio.1181
46. R.M. Richardson, R. Pelton, T. Cosgrove, J. Zhang, A neutron reflectivity study of poly(N-isopropylacrylamide) at the air–water interface with and without sodium dodecyl sulfate. Macromolecules **33**(17), 6269–6274 (2000). https://doi.org/10.1021/ma000095p
47. J. Zhang, R. Pelton, The dynamic behavior of poly (N-isopropylacrylamide) at the air/water interface. Colloids Surf. A **156**(1–3), 111–122 (1999)